

c0040

The Gloria Transform Fault—NE Atlantic: Seismogenic and Tsunamigenic Potential

R. Omira^{*,†}, M. Neres^{*,†}, L. Batista^{*,†}

^{*}Portuguese Institute for Sea and Atmosphere, IPMA, Lisbon, Portugal [†]Dom Luiz Institute, IDL, Faculty of Sciences, University of Lisbon, Lisbon, Portugal

O U T L I N E

1 Introduction	1	5 Discussion	8
2 Geodynamic Setting	3	6 Conclusions	10
3 The Gloria Transform Fault	4	Acknowledgments	10
4 Tsunamigenic Potential of Gloria Fault	6	References	10

s0010

1 INTRODUCTION

p0055

The Azores-Gibraltar fracture zone (AGFZ) marks the western plate boundary between the Eurasian and Nubian plates. It extends eastwards from the Mid-Atlantic Ridge in the Azores toward the Strait of Gibraltar (Fig. 1). The central domain of the AGFZ, called Gloria Fault (GF), follows a prominent morphological feature. The GF was first mapped by Laughton et al. (1972) and presents a relatively slow, ~5mm/year, interplate motion (Fernandes et al., 2003) dominated by dextral strike-slip faulting. Seismically, it is characterized by low seismic activity, although exhibiting a large variation between its eastern, central and western segments. The lack of seismic activity in the eastern GF segment suggests that the low-magnitude earthquakes are probably not detectable by the available seismic network.

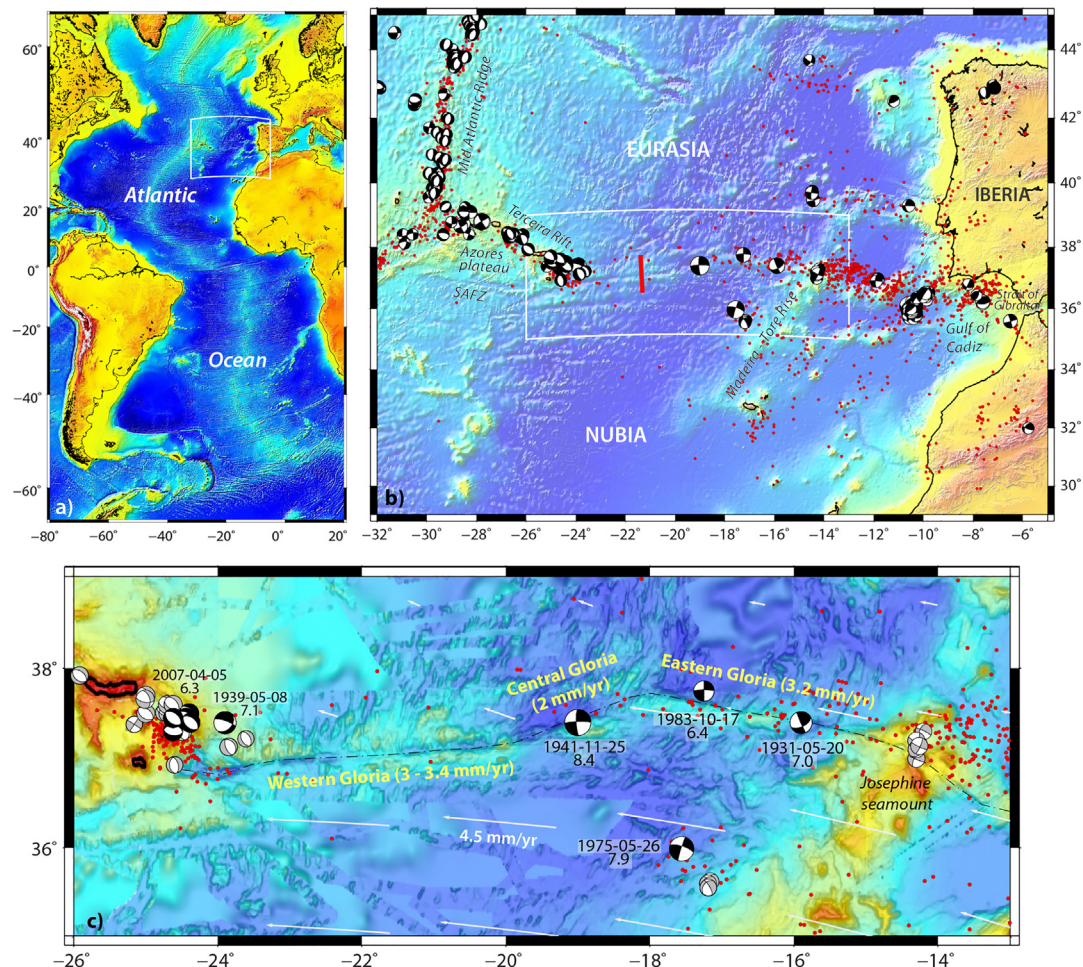


FIG. 1 (A) Location of the study area in the Atlantic Ocean. The Azores-Gibraltar fracture zone (AGFZ) is the only fracture-transform zone in the Atlantic Ocean that constitutes a relatively discrete major plate boundary. (B) The AGFZ and its regional context. *Red dots* are epicenters of $M > 4$ earthquakes from the International Seismological Center (ISC) for the period 1970–2017. Focal mechanisms from the database compiled by Custódio et al. (2016) ($M > 5$). *Red line* locates the seismic refraction and multichannel seismic reflection profiles by Batista et al. (2017) (Fig. 2). SAFZ: South Azores fracture zone. (C) The Gloria Fault. *Red dots*: $M > 4$ epicenters. Focal mechanisms (Custódio et al., 2016 database) for earthquakes $M > 5$ (in gray) and $M > 6$ (in black, labels indicate date and magnitude). *White arrows*: vectors from the relative NU-EU velocity field as modeled by the neotectonic model of Neres et al. (2016). *Yellow labels*: Gloria Fault segments and respective slip rates as inferred by Neres et al. (2016) (note that the model allows for fault slip and continuum strain rate).

Alternatively, this could indicate that the GF in this area is locked and loading for the next big earthquake. This later hypothesis is supported by the occurrence of past large strike-slip earthquake events within the GF or in its proximities.

During the 20th century, three large earthquakes ($M > 7$) took place along the GF or in its proximity (Fig. 1C). All have generated tsunamis that were recorded by the regional

tide-gauge network. The Ms 7.1, May 8, 1939, earthquake occurred near the Azores (see Fig. 1C) with an epicenter located close to the end of the GF (Buform et al., 1988; Reis et al., 2017). It caused a small tsunami that was recorded by the Ponta Delgada (Azores) tide gauge (Reis et al., 2017). On November 25, 1941, an M 8.4 earthquake occurred in the central segment of the GF (see Fig. 1C, Udias et al., 1976; Baptista et al., 2016). It was considered the largest strike-slip event ever recorded (Bird and Kagan, 2004) until the April 11, 2012 Sumatra earthquake, Mw 8.6 (Meng et al., 2012). The 1941 GF earthquake was followed by a tsunami recorded by sea-level stations in Portugal mainland, Morocco, Madeira, and Azores islands, with a maximum wave height of about 0.2 m in Ponta Delgada (Azores) (Baptista et al., 2016). Another high-magnitude event, the M 7.9 May 26, 1975, earthquake had its source 100 km south from the eastern segment of the GF (see Fig. 1C, Buform et al., 1988; Kaabouben et al., 2008). This strike-slip earthquake also generated a small tsunami that was recorded by the Portuguese, Spanish, and the Moroccan tide-gauge networks (Kaabouben et al., 2008). The spatial distribution of these large events suggests that there is no unique discrete structure running from the Azores to Gibraltar that can be considered as the locus of seismic slip, but rather some degree of fault-segment delocalization accounting for the observed earthquake dispersion (Baptista et al., 2017).

p0065 In this chapter, we provide, as a starting point, an overview of the geodynamic setting of the AGFZ. We then focus on the Gloria transform fault by describing the main geometry and interpreted kinematics of this major tectonic structure, as well as its main associated seismicity. Furthermore, we use numerical modeling of tsunami propagation to provide new insight into the tsunamigenesis of the GF, and discuss the implications of its tsunamigenic potential on the NE Atlantic, the Mediterranean, and Connected Seas Tsunami Warning System (NEAM TWS).

2 GEODYNAMIC SETTING

s0015

p0070 The AGFZ is a complex structure bordering Nubia and Eurasia in the Atlantic that underwent a complex tectonic evolution (Fig. 1A and B). It runs from the Azores plateau (in the west) to the Strait of Gibraltar (in the east) across three distinct morphotectonic domains: the Azores triple junction zone, the GF, and the southwest Iberian Margin (SWIM) (Fig. 1B). Within each domain, different kinematic and stress regimes occur, mostly determined by the Nubia-Eurasia (NU-EU) relative motion (e.g., Fernandes et al., 2003; Serpelloni et al., 2007; Neres et al., 2016).

p0075 The Azores triple junction zone is the westernmost domain of the AGFZ where the North American, African (Nubia), and the Eurasian plates meet, and where the NU-EU boundary shows a divergent relative motion (Fig. 1B). This domain comprises a zone of distributed transtensional deformation close to the Mid-Atlantic Ridge that connects to the NW-SE-oriented Terceira spreading ridge (e.g., Miranda et al., 2014, 2015). Along the Terceira Rift, extensional tectonics generate intense normal regime seismicity of low to moderate magnitude that accounts for most of the NU-EU relative motion, also suggested by the absence of seismicity at the South Azores fracture zone (SAFZ, see Fig. 1B).

p0080 The easternmost domain of the AGFZ runs from the Strait of Gibraltar to the Madeira-Tore Rise across the SWIM (Fig. 1B). Here, Nubia and Eurasia show a convergent movement along

an apparently seismically diffuse plate boundary, but with some degree of earthquake clustering. Deformation is characterized by large-scale strain partitioning along differently oriented major dextral strike-slip and thrust faults, as attested by the diversity of focal mechanisms. Most of the active structures are inherited from previous tectonic episodes (e.g., Mesozoic rifting) and were reactivated since the initiation of the Alpine compressive tectonics (e.g., Zitellini et al., 2009; Terrinha et al., 2009).

p0085 The central domain of the AGFZ, comprised between the eastern tip of the Terceira Rift (24°W) and the Josephine seamount in the Madeira-Tore Rise (14°W) (see Fig. 1B and C), is dominated by a prominent morphological feature, the expression of the GF (Fig. 1C) that is generally assumed to constitute a pure transform plate boundary segment.

3 THE GLORIA TRANSFORM FAULT

s0020

p0090 The GF is commonly described as a composite of three main segments (Fig. 1C). Between 24°W and 19°30'W (western Gloria—see Fig. 1C) it strikes parallel to the average direction of NU-EU motion, so this is essentially accommodated by strike-slip faulting (Neres et al., 2016). Between 19°30'W and 18°W (central Gloria—see Fig. 1C) it jogs to ENE-WSW, slightly oblique to the kinematic vectors and likely prone to some dextral transpressive strain. From 18°W to 14°30'W (eastern Gloria—see Fig. 1C) it strikes again parallel to the NU-EU motion. Morphologically, the GF is a 15–20-km wide depression with more than 1 km of vertical offset (Fig. 1C), with E-W elongated basins developed between elongated ridges.

p0095 The crustal structure of the GF has recently been investigated by Batista et al. (2017) across a 150-km-long N-S seismic profile (Fig. 2A). Their interpretation (Fig. 2A) shows that the basins overlying the GF have a maximum depth of ~1 km with steepened bounding fault planes dipping ~75 degrees. This study also evidenced the differences in the bulk sedimentation and tectonic deformation between the north and the south side of the GF, that is, Eurasian and Nubian plates. The northern side of the GF shows evidences of minor tectonic movements (Fig. 2A) and a sequence of north-south trending parallel ridges that deflect to NNE-SSW as we move eastwards. In the southern side of the GF, these ridges are not so pronounced and most of the deformation associated with the GF strike-slip tectonic movement is accommodated there. Moreover, the analysis of wide-angle data, by Batista et al. (2017), has showed a five-layer Vp velocity model (L1–L5 in Fig. 2B). L1 comprises both pelagic sediments and basaltic flows or volcanic sedimentary complex and corresponds to seismo-stratigraphic units U1 + U2 (Fig. 2A); L2 (~3 km thick) presents a basaltic composition normally referred to as oceanic upper crust; L3 (~5 km thick) is in agreement with a gabbroic composition normally referred to as oceanic lower crust; L4 (~4 km thick) was interpreted as partial serpentinization of the upper lithospheric mantle; and L5 corresponds to upper mantle. From this experiment Batista et al. (2017) inferred that the thickness of the crust is ~8 km in the GF strike and ~7 km toward north and south of the GF strike.

p0100 The assumption of the GF as a localized transform plate boundary is challenged by the characteristics of the seismicity record. The seismic events (plotted in Fig. 1) show significant moderate seismic activity in the Azores and SWIM domains but less activity along the Gloria domain. The eastern Gloria is the most active segment, while seismic event is almost absent in

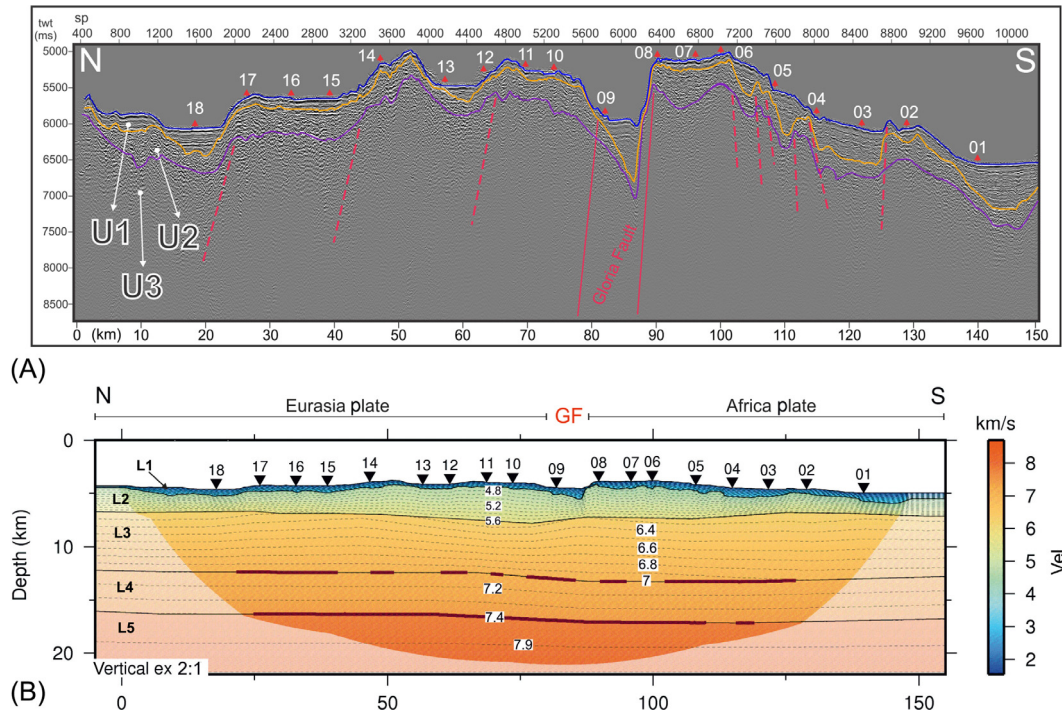


FIG. 2 Morphology and structure across the Gloria Fault, after Batista et al. (2017) (profile located with a red line in Fig. 1). (A) Interpreted MCS profile w51: U1—pelagic sediments interbedded with gravity-driven deposition; U2—volcanic or volcanic-sedimentary complex; U3—magmatic crustal material. (B) Vp velocity model from wide-angle seismic refraction: GF—Gloria Fault; L1–L5—modeled layers; dark red lines show reflected waves. Contours are spaced 0.1 km/s. Numbers and triangles represent positions of OBS.

the western Gloria segment. Moreover, the epicenters of the few recorded earthquakes do not follow the Gloria trend but appear to be spread around it. This may result from inaccurate localization of the events, due to the long distance to the seismic networks, as well as to the low azimuthal coverage of this oceanic area. Nonetheless, three large instrumental strike-slip events (M8.4, M7.0, and M6.4) have been recorded within the Gloria domain and all are located very close to its morphological structure. This suggests that large events/ruptures would preferably localize along the main structure, irrespective of a possible more spread location of the small events. The M8.4 Gloria earthquake of 1941 (Bufo et al., 1988; Baptista et al., 2016) was the largest strike-slip earthquake recorded until the Mw8.6 Sumatra earthquake in 2012. Such a large magnitude might have implied a long rupture propagating for multiple segments, eventually until the western Gloria domain. This large rupture has been evoked as a possible justification for the lack of seismicity on the GF: it may now be locked and loading for a next big event. Another challenging fact for the definition of the GF as a pure transform plate boundary is the 1975 M7.9 strike-slip earthquake (Fig. 1C). This large magnitude event, located about 100 km south of Gloria, in the prolongation of an arguably inactive fracture zone, may suggest that Gloria is not the only active plate boundary

structure along this domain (Baptista et al., 2017). It may rather consist of a plate boundary zone with transform motion distributed among several fracture zones. An alternative explanation for the 1975 event may involve the close presence of the crustal-thickened Madeira-Tore Rise, which certainly affects and deflects the nearby stress and strain fields.

4 TSUNAMIGENIC POTENTIAL OF GLORIA FAULT

s0025

p0105 In this chapter, the evaluation of the tsunamigenic potential of the GF follows a number of steps which include: (i) definition of the tsunami sources; (ii) characterization and parameterization of the maximum credible tsunamigenic scenarios; (iii) modeling of tsunami generation; and (iv) simulation of the tsunami propagation and the resulting coastal wave heights.

p0110 Our definition of the tsunami sources for the GF is based on the available earthquakes information, particularly for the 1941 and 1975 events, and on the recently published works (e.g., Kaabouben et al., 2008; Baptista et al., 2016, 2017; Batista et al., 2017). This leads to distinguish a maximum credible tsunami scenario within each one of the three main GF segments, namely the western GF, the central GF, and the eastern GF. Additionally, a tsunamigenic scenario corresponding to the rupture of a 250-km fault length, located 100 km south of the GF, is also considered to include the fault where the 1975 event may have occurred.

p0115 Table 1 depicts the earthquake fault parameters for the maximum credible scenarios considered in this work. These parameters are used to compute the tsunami generation following the earthquake occurrence.

p0120 To model the generation of the tsunami, we use the Okada's (1985) half-space elastic model to calculate the earthquake-induced sea-bottom coseismic deformation that it is assumed to mimic the sea-surface deformation. Then, we propagate the tsunami from the source to the target coast of the NE Atlantic by solving the nonlinear shallow water equations using staggered-grid finite difference scheme (Omira et al., 2016a; Baptista et al., 2017 and references therein). As the simulation of the tsunami inundation is beyond the scope of this work, we use a coarse resolution bathymetric/topographic grid (800 × 800 m) in our simulations of tsunami propagation. This bathymetric model was generated using multisource height/depth data from the GEBCO 30-arcs gridded data, and from the SWIM bathymetry compilation (Zitellini et al., 2009).

t0010 **TABLE 1** Earthquake Fault Parameters for the Selected Tsunamigenic Scenarios of the GF

Rupture Segment	Max. Mag (Mw)	Length (km)	Width (km)	Slip (m)	Strike (°)	Dip (°)	Rake (°)
Western GF	8.6	300	45	10	265	75	161
Central GF	8.4	200	45	8	255	88	161
Eastern GF	8.4	200	45	8	282	88	161
1975-Fault	8.5	250	45	8	277	88	161

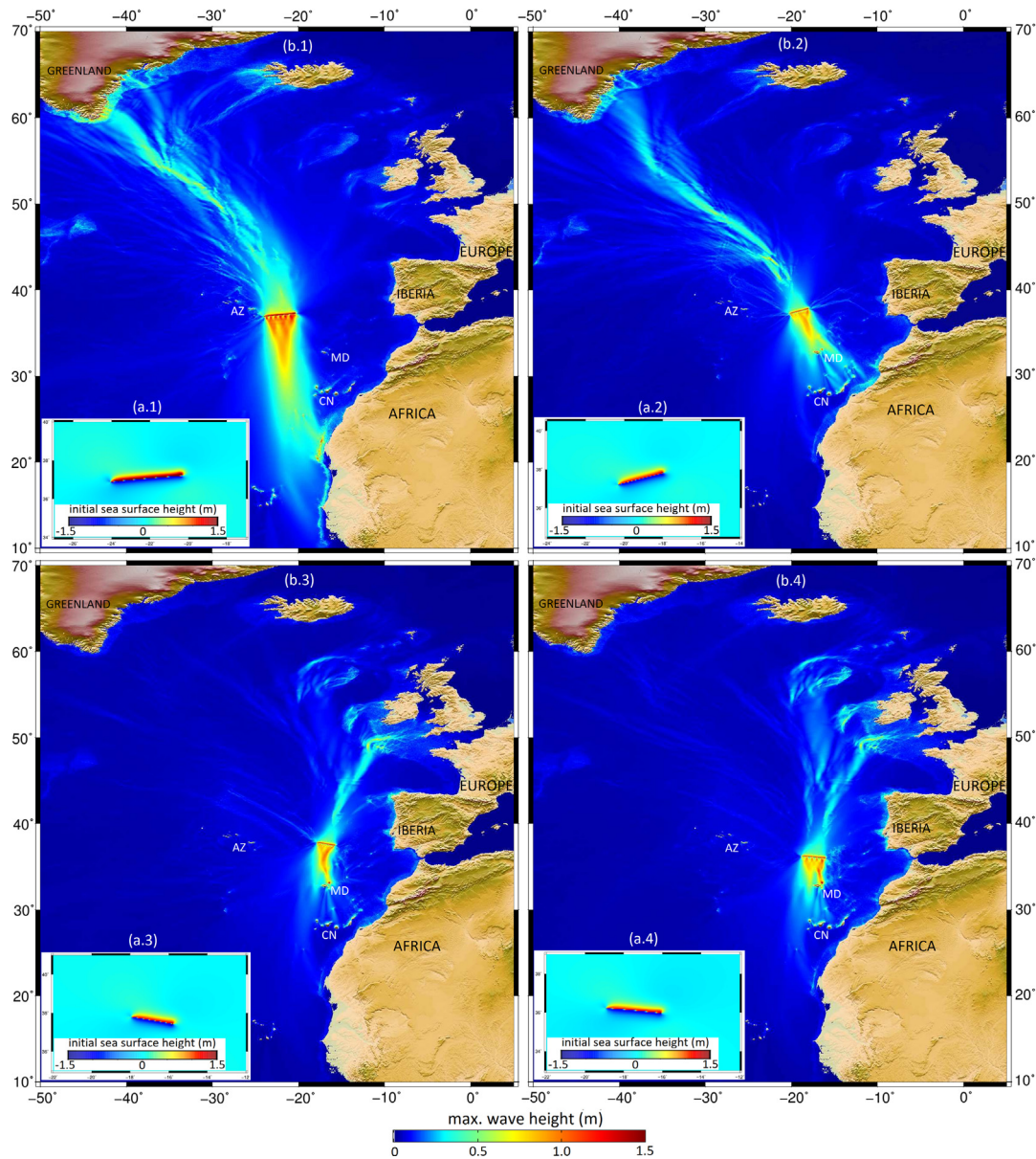


FIG. 3 Tsunami numerical models for the four-selected maximum credible earthquake scenarios of the GF. (A) The initial sea-surface perturbations that follow the sea-bottom coseismic deformations from: (1) the western GF, (2) the central GF, (3) the eastern GF, and (4) the 1975-fault earthquake scenarios. (B) The maximum tsunami wave heights distributions in the NE Atlantic region from: (1) the western GF, (2) the central GF, (3) the eastern GF, and (4) the 1975-fault tsunami scenarios. AZ, Azores; CN, Canary Islands; MD, Madeira.

- p0125 **Fig. 3** depicts the tsunami models for the maximum credible earthquake scenarios of the GF. The analysis of the initial sea-surface perturbation (**Fig. 3A1–4**) clearly shows that the Mw8.4–8.6 GF earthquakes lead to the generation of relatively small tsunamis, with maximum wave heights in the range of 0.8–1.2 m. This is mainly due to the mechanism of the earthquake ruptures, which are mainly dominated by a strike-slip motion, causing a small vertical deformation of the sea bottom.
- p0130 The tsunamis from the GF's maximum credible earthquake scenarios pose a low threat along the most of the NE Atlantic coast (**Fig. 3B, 1–4**). Results of maximum wave heights computations show values of less than 1 m (**Fig. 3**). They are in good agreement with the observed tsunami heights from the past events in the region ([Kaabouben et al., 2008](#); [Baptista et al., 2016, 2017](#)). The tsunami energy distribution from the selected scenarios meets the reasonable expectations, being, at first order, maximal in the direction perpendicular to the fault strike. However, when the tsunami propagates away from the source it encounters shallow water zones that affects its waveforms and amplifies its wave heights. For such a reason, we observe the effect of the Mid-Atlantic Ridge bathymetry channeling the tsunami energy (**Fig. 3B, 1 and 2**) which results in a noticeable impact along the coast of Greenland, even though it is located far from the source zone.
- p0135 Results also show that the location of the earthquake source within the GF can help identify the coastal regions that are mostly threatened by a potential tsunami. The Mw8.6 eastern GF scenario steers most of the tsunami energy toward the Azores and Greenland coasts, with a maximum wave height of up to 0.8 m (**Fig. 3B, 1**), whereas, only small waves, less than 0.25 m, reach the Iberian coast. Moving westward, the coasts of Madeira and Canary Islands are the most affected by the Mw8.4 event generated on the central GF segment. Simulated maximum wave heights along Madeira's northern coast are in the range of 1 m (**Fig. 3B, 2**). Both the eastern GF and the 1975-fault scenarios, Mw8.4 and Mw8.5 respectively, are the most effective in steering tsunami energy toward the Iberian and African coasts. However, the incident tsunami remains relatively small with waves up to 0.4 m in height.

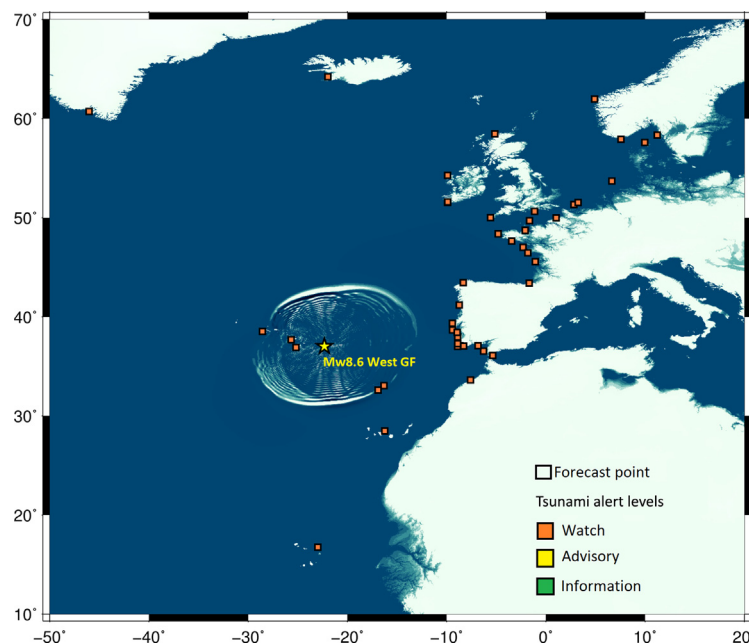
5 DISCUSSION

- s0030
- p0140 The tsunamigenic potential of the GF has been studied in a number of recent works ([Omira et al., 2015, 2016b](#); [Baptista et al., 2017](#)). [Omira et al. \(2015, 2016b\)](#) considered the GF as one of the main tsunamigenic source zones in the NE Atlantic to derive probabilistic tsunami hazard maps at regional and local scales. [Baptista et al. \(2017\)](#) produced a tsunami catalog using an earthquake synthetic catalog compatible with the plate kinematic constraints of the area. This work, on the other hand, focuses on the tsunamigenesis of the GF from the perspective of the maximum credible earthquake scenarios. While the approach used here is considered the simplest, in comparison to the previously mentioned works, the outcomes of this chapter are easy to interpret and, therefore, can better serve the tsunami warning purpose in the NE Atlantic.
- p0145 Understanding how tsunamis are generated in the GF domain and propagated toward the NE Atlantic coast helps decision makers in the tsunami warning centers (TWCs) to determine how future tsunamis in the region can be mitigated. In the NE Atlantic region, TWCs use the

Tsunami Decision Matrix (TDM), proposed by the ICG/NEAMTWS (Intergovernmental Co-ordination Groups/NEAMTWS), to quickly forecast the tsunami threat from large earthquakes. The TDM is an easy-to-use table establishing a link between the earthquake parameters and the possible ensuing tsunami. However, the fact that the TDM only considers the basic earthquake parameters (location, magnitude, and depth) without any information on the rupture mechanism limits the effectiveness of this tool.

p0150 To examine the adequacy of the TDM for the potentially tsunamigenic earthquakes of the GF, we compared its performance with the numerical model for the proposed scenario (Fig. 4). For the Mw8.6 western GF scenario, the TDM leads to the maximum tsunami warning level, that is, “Watch,” for the entire NE Atlantic coast, which is in disagreement with the numerical modeling results that show only very small tsunami waves along most of the coastal zones of the region. This comparison clearly indicates that the NEAMTWS’s TDM overestimate the tsunami threat from the large earthquakes of the GF. This suggests a review of the TDM tool to reduce probable false warning following the GF earthquakes.

p0155 [Tinti et al. \(2012\)](#) have investigated the applicability of the TDM to the Italian tsunamis and reached similar conclusions on the need of substantial improvements in this forecast tool to meet early warning requirements. Moreover, they proposed diverse ways of TDM improvements including: (1) to keep the concept as it is and perform a sensitivity analysis to define the boundaries that provide the best performance; (2) integrate additional earthquake parameters, such as the focal mechanism; (3) discard the concept of the TDM and use the



f0025 **FIG. 4** Application of the Tsunami Decision Matrix for the Mw 8.6 western GF scenario and the resulting tsunami warning levels at the official forecast points along the NE Atlantic coasts.

precomputed scenarios database to forecast earthquake-induced tsunamis. These propositions can form the basis for a further review of the TDM in the NE Atlantic region.

6 CONCLUSIONS

s0035

p0160 This chapter presents an overview of the seismogenic and tsunamigenic potential of the
p0165 GF, a domain of the AGFZ that marks the western Eurasia-Nubia plate boundary.

p0165 The following main conclusions are drawn:

- o0050 1. The GF is underexplored, and substantial further work is needed to understand its general
tectonic framework and evolution.
- o0055 2. Despite the lack of recorded seismic activity in some parts of the GF, the occurrence of large
seismic events favors the hypothesis that GF is locked and loading for the next big
earthquake.
- o0060 3. Tsunamis from the GF pose low hazard for most of the NE Atlantic coasts.
- o0065 4. The forecast procedure in-use at the TWCs of the NE Atlantic region overestimates the
tsunami threat from the GF.

Acknowledgments

This work was supported by the project ASTARTE—Assessment, STRategy And Risk Reduction for Tsunamis in Europe, Grant 603839, 7th FP (ENV.2013.6.4-3), and by the FCT project UID/GEO/50019/2013, Instituto Dom Luiz. Portuguese Task Group for the Extension of the Continental Shelf (EMEPC) is thanked for making available the high-resolution multibeam bathymetry around the GF. The authors wish to thank the Editor João Duarte and the Reviewer Filipe Rosas for their timely reviews, which improved the manuscript.

References

- Baptista, M.A., Miranda, J.M., Batlló, J., Lisboa, F., Luis, J., Maciá, R., 2016. New study on the 1941 Gloria Fault earthquake and tsunami. *Nat. Hazards Earth Syst. Sci.* 16 (8), 1967–1977.
- Baptista, M.A., Miranda, J.M., Matias, L., Omira, R., 2017. Synthetic tsunami waveform catalogs with kinematic constraints. *Nat. Hazards Earth Syst. Sci.* 17 (7), 1253.
- Batista, L., Hübscher, C., Terrinha, P., Matias, L., Afilhado, A., Lüdmann, T., 2017. Crustal structure of the Eurasia–Africa plate boundary across the Gloria Fault, North Atlantic Ocean. *Geophys. J. Int.* 209, 713–729.
- Bird, P., Kagan, Y.Y., 2004. Plate-tectonic analysis of shallow seismicity: apparent boundary width, beta, corner magnitude, coupled lithosphere thickness, and coupling in seven tectonic settings. *Bull. Seismol. Soc. Am.* 94 (6), 2380–2399.
- Bufo, E., Udias, A., Colombas, M.A., 1988. Seismicity, source mechanisms and tectonics of the Azores-Gibraltar plate boundary. *Tectonophysics* 152 (1–2), 89–118.
- Custódio, S., Lima, V., Vales, D., Cesca, S., Carrilho, F., 2016. Imaging active faulting in a region of distributed deformation from the joint clustering of focal mechanisms and hypocentres: application to the Azores–western Mediterranean region. *Tectonophysics* 676, 70–89.
- Fernandes, R., Ambrosius, B.A.C., Noomen, R., Bastos, M., Wortel, M., Spakman, W., Govers, R., 2003. The Relative Motion Between Africa and Eurasia as Derived From ITRF2000 and GPS Data. *Geophys. Res. Lett.* 30, 1828.
- Kaoubou, F., Brahim, A.I., Toto, E., Baptista, M.A., Miranda, J.M., Soares, P., Luis, J.F., 2008. On the focal mechanism of the 26.05.1975 North Atlantic event contribution from tsunami modeling. *J. Seismol.* 12, 575–583.

- Laughton, A.S., Whitmarsh, R.B., Rusby, J.S.M., Somers, M.L., Revie, J., McCartney, B.S., Nafe, J.E., 1972. A continuous east west fault on the Azores-Gibraltar Ridge. *Nature* 237, 217–220. <https://doi.org/10.1038/237217a0>.
- Meng, L., Ampuero, J.P., Stock, J., Duputel, Z., Luo, Y., Tsai, V.C., 2012. Earthquake in a maze: compressional rupture branching during the 2012 Mw 8.6 Sumatra earthquake. *Science* 337 (6095), 724–726.
- Miranda, J.M., Luis, J.F., Lourenço, N., Goslin, J., 2014. Distributed deformation close to the Azores Triple “Point” Mar. Geol. 355, 27–35.
- Miranda, J.M., Luis, J.F., Lourenço, N., Fernandes, R.M.S., 2015. The structure of the Azores Triple Junction: implications for São Miguel Island. In: Geological Society, London, Memoirs. vol. 44, pp. 5–13. <https://doi.org/10.1144/M44.2> (Chapter 2).
- Neres, M., Carafa, M.M.C., Fernandes, R.M.S., Matias, L., Duarte, J.C., Barba, S., Terrinha, P., 2016. Lithospheric deformation in the Africa-Iberia plate boundary: improved neotectonic modeling testing a basal-driven Alboran plate. *J. Geophys. Res. Solid Earth* 121, 6566–6596.
- Okada, Y., 1985. Surface deformation due to shear and tensile faults in a half-space. *Bull. Seismol. Soc. Am.* 75 (4), 1135–1154.
- Omira, R., Baptista, M.A., Matias, L., 2015. Probabilistic tsunami hazard in the Northeast Atlantic from near-and far-field tectonic sources. *Pure Appl. Geophys.* 172 (3–4), 901–920.
- Omira, R., Baptista, M.A., Lisboa, F., 2016a. Tsunami characteristics along the Peru–Chile trench: analysis of the 2015 Mw8. 3 Illapel, the 2014 Mw8. 2 Iquique and the 2010 Mw8. 8 Maule tsunamis in the near-field. *Pure Appl. Geophys.* 173 (4), 1063–1077.
- Omira, R., Matias, L., Baptista, M.A., 2016b. Developing an event-tree probabilistic tsunami inundation model for NE Atlantic coasts: application to a case study. *Pure Appl. Geophys.* 173 (12), 3775–3794.
- Reis, C., Omira, R., Matias, L., Baptista, M.A., 2017. On the source of the 8 May 1939 Azores earthquake–tsunami observations and numerical modelling. *Geomat. Nat. Hazards Risk* 8 (2), 328–347.
- Serpelloni, E., Vannucci, G., Pondrelli, S., Argnani, A., Casula, G., Anzidei, M., Baldi, P., Gasperini, P., 2007. Kinematics of the Western Africa-Eurasia plate boundary from focal mechanisms and GPS data. *Geophys. J. Int.* 169, 1180–1200.
- Terrinha, P., Matias, L., Vicente, J., Duarte, J., Luís, J., Pinheiro, L., Lourenço, N., Diez, S., Rosas, F., Magalhães, V., Valadares, V., Zitellini, N., Roque, C., Víctor, L.M., 2009. Morphotectonics and strain partitioning at the Iberia-Africa plate boundary from multibeam and seismic reflection data. *Mar. Geol.* 267, 156–174.
- Tinti, S., Graziani, L., Brizuela, B., Maramai, A., Gallazzi, S., 2012. Applicability of the decision matrix of North Eastern Atlantic, Mediterranean and connected seas Tsunami Warning System to the Italian tsunamis. *Nat. Hazards Earth Syst. Sci.* 12, 843–857.
- Udias, A., Arroyo, A.L., Mezcuca, J., 1976. Seismotectonic of the Azores-Alboran region. *Tectonophysics* 31 (3–4), 259–289.
- Zitellini, N., Gràcia, E., Matias, L., Terrinha, P., Abreu, M.A., DeAlteriis, G., Henriët, J.P., Dañobeitia, J.J., Masson, D.G., Mulder, T., Ramella, R., Somoza, L., Diez, S., 2009. The quest for the Africa-Eurasia plate boundary west of the Strait of Gibraltar. *Earth Planet. Sci. Lett.* 280, 13–50.

B978-0-12-812064-4.00008-6, 00008

Duarte, 978-0-12-812064-4

Non-Print Items

Abstract

The Gloria Fault (GF) is a large transform segment of the Azores-Gibraltar fracture zone (AGFZ) marking the Eurasia-Nubia plate boundary in the NE Atlantic. We first provide an overview of the geodynamic setting of the AGFZ with a special emphasis on the GF, its structure, seismic activity, and tsunamigenic potential. We then present a quantitative assessment of the tsunamigenesis of the GF through numerical modeling of past tsunami events and associated possible scenarios. We found that despite the potential of the GF to generate high-magnitude earthquakes, the ensuing tsunami hazard remains low to moderate. This suggests a review of the tool used to forecast tsunamis (Tsunami Decision Matrix) in this specific region of the NE Atlantic.

Keywords: Gloria Fault, Azores-Gibraltar fracture zone, Tsunamigenic potential